

Two loop QCD corrections to $e^+e^- \rightarrow J/\psi + \eta_c$ in asymptotic expansion

Cong Li*,¹ Xu-Dong Huang^{†,2} and Wen-Long Sang^{‡1}

¹*School of Physical Science and Technology,
Southwest University, Chongqing 400700, China*

²*College of Physics and Electronic Engineering,
Chongqing Normal University, Chongqing 401331, China*

(Dated: June 23, 2025)

Abstract

Within the framework of NRQCD, the short-distance coefficients (SDCs) for the process $e^+e^- \rightarrow J/\psi + \eta_c$ have been obtained up to NNLO in asymptotic expansions over $r = 16m_c^2/s$ up to r^{15} . Although these asymptotic expressions are deviated from the full results near the threshold $r = 1$, they provide excellent approximations to the full results for $r < 0.8$, with deviations less than 3%. Therefore, these asymptotic expressions offer reliable applications for phenomenological predictions across a wide range of center-of-mass energies \sqrt{s} . Utilizing these asymptotic expressions, we present phenomenological predictions for the cross sections in both the on-shell mass scheme and the $\overline{\text{MS}}$ mass scheme, with the uncertainty arising from the renormalization scale μ_R included. The μ_R uncertainty for predictions from the $\overline{\text{MS}}$ mass scheme is slightly larger than that from the on-shell mass scheme, which is partly attributed to the helicity flip in the process $e^+e^- \rightarrow J/\psi + \eta_c$. We observe that both mass schemes yield quite similar predictions, and our theoretical results are consistent with the available experimental data.

PACS numbers:

* lc312321@163.com

† huangxd@cqu.edu.cn

‡ wlsang@swu.edu.cn

I. INTRODUCTION

The production of double charmonium states in electron-positron annihilation processes, exemplified by the notable process $e^+e^- \rightarrow J/\psi + \eta_c$, provides an ideal platform to explore both the perturbative and non-perturbative nature of QCD. The process $e^+e^- \rightarrow J/\psi + \eta_c$ was first measured by the BELLE collaboration, yielding $\sigma_{e^+e^- \rightarrow J/\psi + \eta_c} \times B_{\geq 4} = 33_{-6}^{+7} \pm 9$ fb [1], which was later revised to $\sigma_{e^+e^- \rightarrow J/\psi + \eta_c} \times B_{>2} = 25.6 \pm 2.8 \pm 3.4$ fb [2]. Here $B_{>n}$ denotes the branching fraction of η_c decaying into n charged tracks. In 2005, an independent measurement by the BABAR collaboration reported $\sigma_{e^+e^- \rightarrow J/\psi + \eta_c} \times B_{>2} = 17.6 \pm 2.8_{-2.1}^{+1.5}$ fb [3]. Recently, the BELLE collaboration conducted further searches for this process at the $\Upsilon(nS)$ ($n = 1-5$) on resonance and 10.52 GeV off-resonance energy points, but no significant signal of the double charmonium state is found [4].

These experimental measurements have sparked a flurry of theoretical investigations in the following years [5–31]. The NRQCD factorization [32] has emerged as a cornerstone for describing the process $e^+e^- \rightarrow J/\psi + \eta_c$. Leading-order (LO) NRQCD predictions were initially carried out in Refs. [5, 6, 8, 12], but these were found to be an order of magnitude smaller than the experimental measurements. A significant breakthrough came with the calculation of the next-to-leading order (NLO) radiative corrections, which were substantial and positive, significantly reducing the discrepancy between theory and experiment [13, 20]. Meanwhile, both $\mathcal{O}(v^2)$ and $\mathcal{O}(\alpha_s v^2)$ corrections were also explored [5, 17, 23, 26].

Very recently, the notable next-to-next-to-leading-order (NNLO) radiative corrections were first numerically evaluated in Ref. [31] and later verified in Ref. [28]. These corrections were found to be considerable. While the inclusion of all radiative and relativistic corrections brings the theoretical prediction into consistency with the experimental measurement [31], significant uncertainties remain from the renormalization scale and the charm quark mass, which undermine the clarity of this agreement.

More serious, it has been noted that the renormalized pole mass is subject to a non-perturbative renormalon ambiguity of $\mathcal{O}(\Lambda_{\text{QCD}})$ [33–35], which not only affects the definition of the pole mass but also potentially impacts the perturbative expansion of the cross section. In contrast, the short-distance $\overline{\text{MS}}$ mass is expected to be free from such ambiguities. The conversion from the on-shell (OS) mass scheme to the $\overline{\text{MS}}$ mass scheme for the cross section is straightforward only if the analytic expression of the cross section is known. Additionally, it has been found that the leading logarithmic term $\ln^2 r$ dominates the NLO radiative corrections [25, 36]. Whether large logarithmic terms will also dominate the NNLO corrections remains unknown. If an analytic expression can be derived, it will not only address this question but also facilitate the resummation of large logarithms. Moreover, the analytic expression will greatly facilitate phenomenological applications, particularly when different center-of-mass (CM) energies \sqrt{s} or charm quark masses are considered.

Unfortunately, it seems insurmountable to derive the analytic expression for the cross section of $e^+e^- \rightarrow J/\psi + \eta_c$ due to the extremely complicated topology in the Feynman diagrams. Thus, our task in this work is to obtain the asymptotic expansion over $r = 16m_c^2/s$. This asymptotic expression includes various logarithmic terms and provides a good approximation of the full results over a wide range of r . Therefore, it allows us to easily convert the theoretical prediction from the OS mass scheme to the $\overline{\text{MS}}$ mass scheme and make other phenomenological predictions.

The overall structure of this paper is summarized as follows. In Sec. II, we express the cross sections in terms of the electromagnetic form factor (FF) and provide the NRQCD

factorization formula for this FF. In Sec. III, we present the theoretical framework and computational methods employed to calculate the short-distance coefficients (SDCs). In Sec. IV, we briefly describe the $\overline{\text{MS}}$ mass scheme. The convergence behavior of the asymptotic expansion of the FF is discussed in Sec. V. Sec. VI is devoted to the phenomenological analysis and discussion. In Sec. VII, we summarize our conclusion. The coefficients of the asymptotic expansion up to r^3 are presented in Appendices A and B.

II. NRQCD FACTORIZATION FOR THE FF AND CROSS SECTION

The cross section for the process $e^+e^- \rightarrow J/\psi + \eta_c$ can be expressed in terms of the time-like electromagnetic (EM) form factor $F(s)$, which is defined via

$$\langle J/\psi(P_1, \lambda) + \eta_c(P_2) | J_{\text{EM}}^\mu | 0 \rangle = i F(s) \epsilon^{\mu\nu\rho\sigma} P_{1\nu} P_{2\rho} \epsilon_\sigma^*(\lambda), \quad (1)$$

where J_{EM}^μ denotes the EM current, P_1 and P_2 are the momenta of the J/ψ and η_c respectively, $s = (P_1 + P_2)^2$, and ϵ represents the polarization vector of J/ψ with $\lambda = \pm 1$ indicating the its helicities.

Within the NRQCD factorization framework [32], the EM form factor $F(s)$ can be expressed as

$$F(s) = \sqrt{2M_{J/\psi}} \sqrt{2M_{\eta_c}} \frac{\langle J/\psi | \psi^\dagger \boldsymbol{\sigma} \cdot \boldsymbol{\epsilon} \chi | 0 \rangle}{m_c} \frac{\langle \eta_c | \psi^\dagger \chi | 0 \rangle}{m_c} \times f, \quad (2)$$

where ψ and χ^\dagger are Pauli spinor fields annihilating a heavy quark and antiquark, respectively. The SDC f encodes the perturbatively calculable physics, while non-perturbative long-distance effects are described by long-distance matrix elements (LDMEs). The prefactor $\sqrt{2M_{J/\psi}} \sqrt{2M_{\eta_c}}$ arises from the relativistic normalization of quarkonium states in the helicity amplitude and their non-relativistic normalization in LDMEs. Additionally, the charm quark mass m_c , which originates from the perturbative matching, has been explicitly factored out in (2).

The cross section is then readily obtained:

$$\begin{aligned} \sigma[e^+e^- \rightarrow J/\psi + \eta_c] &= \frac{4\pi\alpha^2}{3} \left(\frac{|\mathbf{P}_1|}{\sqrt{s}} \right)^3 |F(s)|^2 \\ &= \frac{16\pi\alpha^2 M_{J/\psi} M_{\eta_c} |\mathbf{P}_1|^3}{3s^{\frac{3}{2}}} \frac{\langle \mathcal{O} \rangle_{J/\psi}}{m_c^2} \frac{\langle \mathcal{O} \rangle_{\eta_c}}{m_c^2} |f|^2, \end{aligned} \quad (3)$$

where we have used the shorthand notations $\langle \mathcal{O} \rangle_{J/\psi} = |\langle J/\psi | \psi^\dagger \boldsymbol{\sigma} \cdot \boldsymbol{\epsilon}_{J/\psi} \chi | 0 \rangle|^2$ and $\langle \mathcal{O} \rangle_{\eta_c} = |\langle \eta_c | \psi^\dagger \chi | 0 \rangle|^2$. The magnitude of \mathbf{P}_1 is determined by

$$|\mathbf{P}_1| = \frac{\lambda^{\frac{1}{2}}(s, M_{J/\psi}^2, M_{\eta_c}^2)}{2\sqrt{s}}, \quad (4)$$

with $\lambda(x, y, z) = x^2 + y^2 + z^2 - 2(xy + xz + yz)$.

Note that, we employ the physical masses of the J/ψ and η_c for the variables $M_{J/\psi}$ and M_{η_c} in the cross section (3). These masses stem from the normalization of the states, phase space factors, or the Lorentz contraction arising from Eq. (1). This choice helps to

mitigate theoretical uncertainties associated with the uncertainty in the charm quark mass m_c . Conversely, in the computation of f , we take the masses of the J/ψ and η_c to be $2m_c$.

To obtain the cross section, it is crucial to calculate the SDC f , which can generally be expanded in powers of α_s :

$$f(r) = f^{(0)}(r) \left[1 + \frac{\alpha_s}{\pi} \left(\frac{\beta_0}{4} \ln \frac{4\mu_R^2}{s} + f^{(1)}(r) \right) + \frac{\alpha_s^2}{\pi^2} \left(\frac{\beta_0^2}{16} \ln^2 \frac{4\mu_R^2}{s} + \left(\frac{\beta_1}{16} + \frac{\beta_0}{2} f^{(1)}(r) \right) \ln \frac{4\mu_R^2}{s} + (\gamma_{J/\psi} + \gamma_H) \ln \frac{\mu_\Lambda^2}{m_c^2} + f^{(2)}(r) \right) + \mathcal{O}(\alpha_s^3) \right], \quad (5)$$

where $f^{(0)}$ denotes the LO SDC, $\beta_0 = \frac{11}{3}C_A - \frac{4}{3}T_F n_f$ and $\beta_1 = \frac{34}{3}C_A^2 - (\frac{20}{3}C_A + 4C_F)T_F n_f$ are the one-loop and two-loop coefficients of the QCD β function respectively, and $n_f = n_l + n_h$ represents the number of active flavors, with $n_l=3$ being the number of light quarks, and $n_h = 1$ the number of heavy quark.

μ_R and μ_Λ refer to the renormalization scale and the NRQCD factorization scale, respectively. The $\ln \mu_R^2$ terms ensure the renormalization group invariance of the SDCs, while the occurrence of $\ln \mu_\Lambda^2$ is required by the NRQCD factorization. According to the factorization, the μ_Λ -dependence in the SDCs should be completely eliminated by that in the LDMEs. The anomalous dimensions $\gamma_{J/\psi}$ and γ_{η_c} associated with the NRQCD bilinear currents carrying the quantum numbers 3S_1 and 1S_0 are given by [37–39]

$$\gamma_{J/\psi} = -\pi^2 \left(\frac{C_A C_F}{4} + \frac{C_F^2}{6} \right), \quad (6)$$

$$\gamma_{\eta_c} = -\pi^2 \left(\frac{C_A C_F}{4} + \frac{C_F^2}{2} \right). \quad (7)$$

The $f^{(0)}(r)$ and $f^{(1)}(r)$ have been known for some time [5, 13, 20]. Recently, the numerical values of $f^{(2)}(r)$ at certain special CM energies have been determined [28, 31]. Instead of tackling the challenging task of deriving the full analytic expressions for $f^{(2)}(r)$, our goal in this work is to perform an asymptotic expansion in r and present the asymptotic expressions for $f^{(2)}$. We expect that these asymptotic expressions will provide good approximations to the full results over a wide range of r , making them suitable for both theoretical analysis and phenomenological calculations.

III. THEORETICAL FRAMEWORK AND COMPUTATIONAL METHODS

To compute the SDCs, we take a direct approach by calculating the quark-level amplitude for the process $\gamma^* \rightarrow c\bar{c}(^3S_1^{(1)}, P_1) + c\bar{c}(^1S_0^{(1)}, P_2)$. We utilize **FeynArts** [40] to generate the Feynman diagrams and corresponding amplitudes for $\gamma^* \rightarrow c\bar{c}(^3S_1^{(1)}) + c\bar{c}(^1S_0^{(1)})$. Some typical Feynman diagrams are illustrated in Fig. 1.

The two-loop diagrams can be categorized into two main types: the regular part and the “light-by-light” (lbl) part. The latter features a unique topology where a closed quark loop is connected to the time-like photon and three gluons. Given that the sum of the electric charges of the light flavors cancels out, e.g., $\sum_{q=u,d,s} e_q = 0$, we can safely ignore the lbl contributions from the light quark loops.

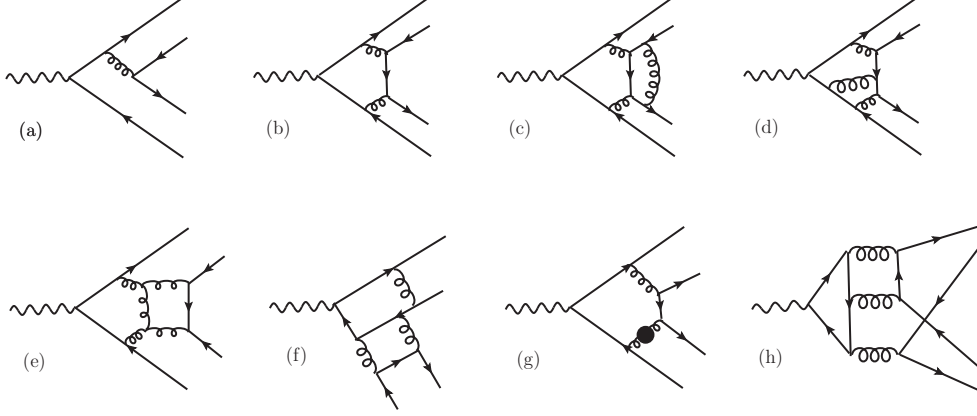


FIG. 1: Some typical Feynman diagrams for the process $\gamma^* \rightarrow c\bar{c}(^3S_1^{(1)}) + c\bar{c}(^1S_0^{(1)})$ are illustrated. (a) and (b) represent the LO and NLO diagrams, respectively. (c) to (h) correspond to the NNLO contributions. The final diagram (h) illustrates the “light-by-light” part.

We employ the packages **FeynCalc** and **FormLink** [41, 42] to perform Lorentz contractions and Dirac algebra. To LO accuracy in v , we neglect the relative momentum in each $c\bar{c}$ pair prior to carrying out the loop integration. This approach allows us to directly extract the NRQCD SDCs from the hard region [43].

We use **CalcLoop** [44] to classify the Feynman integrals into different families and employ **Kira** [45], **Blade** [46], and **FIRE** [47] to perform integration-by-parts (IBP) reductions. This process yields approximately 500 master integrals (MIs) across 80 families. We work in $d = 4 - 2\epsilon$ spacetime dimensions to regularize both UV and IR divergences.

We will derive the asymptotic expressions for the MIs as $r \rightarrow 0$ by setting up and solving the differential equations (DEs) that these integrals satisfy with respect to the kinematic variable r . Specifically, we consider a complete set of MIs, denoted by \vec{J} , within a Feynman integral family. These MIs obey the following system of DEs:

$$\frac{\partial}{\partial r} \vec{J} = M(r, \epsilon) \vec{J}, \quad (8)$$

where the matrix M has been transformed into a local Fuchsian form at all singular points, particularly at $r = 0$. The form of the (8) allows us to solve the \vec{J} via series expansion in r . The general form of the asymptotic expansion is given by

$$\vec{J} = \sum_{\rho \in S} r^\rho \sum_{n=0}^{\infty} \vec{C}_\rho(\epsilon) r^n, \quad (9)$$

where S is a finite set of powers that depend on ϵ . The set of exponents ρ can be determined by solving the characteristic equation

$$\det(\rho I - M) = 0, \quad (10)$$

with I representing the identity matrix. The coefficients \vec{C} can then be determined through recurrence relations with the initial conditions.

In our practical computations, we employ a numerical fitting strategy. We first solve the DEs for specific numerical values of ϵ , and subsequently fit the powers ρ and the coefficients \vec{C} as expansions of ϵ by solving systems of linear equations. This approach is implemented using the package auxiliary mass flow [48–50].

Ultimately, we obtain the expressions for each MI. After expanding the MIs in powers of ϵ , we express the MIs at each ϵ -order as

$$\sum_{m,n} c_{m,n} r^m \ln^n r. \quad (11)$$

In this work, we truncate the expansions in r up to r^{15} , which is sufficient to accurately reproduce the full results for a wide range of r . Given the high precision of the coefficients $c_{m,n}$, we utilize the PSLQ algorithm to reconstruct their analytic expressions. We have successfully reconstructed the analytic coefficients up to $\ln^2 r$ for some lower powers of r . While it is feasible to reconstruct all $c_{m,n}$ terms, this would require higher numerical precision and, consequently, additional computational resources.

In this study, the on-shell scheme is employed to renormalize the charm quark mass and field strength, while the $\overline{\text{MS}}$ scheme is utilized for the QCD coupling constant. The renormalized NNLO QCD amplitude retains a single IR pole. However, the coefficient of this pole exactly matches half the sum of the anomalous dimensions for the NRQCD bilinear operators that carry the quantum numbers of J/ψ [37, 38] and η_c [39]. This behavior is precisely anticipated within the framework of NRQCD factorization for double charmonium production at NNLO. Under the $\overline{\text{MS}}$ scheme, this IR pole factorizes into the corresponding NRQCD matrix elements.

After performing a series of intricate calculations, we have successfully derived the expressions for $f^{(n)}$ with $n = 0, 1, 2$.

The LO SDC has long been established in the literature [5]:

$$f^{(0)} = \frac{256\pi\alpha_s m_c}{27s^2}, \quad (12)$$

where m_c arises due to the helicity flip in the process $e^+e^- \rightarrow J/\psi + \eta_c$.

We express $f^{(1)}(r)$ and $f^{(2)}(r)$ in terms of an asymptotic expansion over r :

$$f^{(n)}(r) = \sum_{i,j \geq 0} f_{i,j}^{(n)} r^i \ln^j r, \quad (13)$$

where j ranges from 0 to $2n$, and i can in principle extend to infinity. As mentioned, we have truncated the sum for i at 15.

The expressions for various $f_{i,j}^{(n)}$ up to r^3 are presented in Appendices A and B. The asymptotic expressions for $f^{(1)}(r)$ and $f^{(2)}(r)$, along with the analytic expression for $f^{(1)}(r)$, are included in an attached file. Additionally, $f^{(2)}(r)$ is numerically evaluated at 619 different values of r ranging from 0 to 1, using a strategy analogous to the one described in Refs. [28, 51, 52]. These numerical values are also included in the attached file.

IV. $\overline{\text{MS}}$ MASS SCHEME

It has been noted that the renormalized pole mass is subject to a non-perturbative renormalon ambiguity of $\mathcal{O}(\Lambda_{\text{QCD}})$ [33–35]. In fact, this renormalon ambiguity not only affects

the definition of the pole mass but also potentially impacts the perturbative expansion of the cross section. On the other hand, the short-distance mass, exemplified by the $\overline{\text{MS}}$ mass, has frequently been employed to predict physical quantities in the literature. The $\overline{\text{MS}}$ mass is expected to be free from non-perturbative ambiguities.

Therefore, it is intriguing to discuss the translation of our prediction for the FF from the OS mass scheme to the $\overline{\text{MS}}$ mass scheme.

Given the asymptotic expressions of $f(r)$, the translation can be readily achieved by employing the OS- $\overline{\text{MS}}$ mass relation

$$m_c = \overline{m}_c(\mu_m) \left(1 + \sum_{n=1}^{\infty} \left(\frac{\alpha_s(\mu_m)}{\pi} \right)^n d^{(n)}(\mu_m) \right), \quad (14)$$

where the coefficients $d^{(k)}(\mu_m)$ have been known up to the fourth order [53–57]. For our purposes, only the first two lower orders are necessary:

$$d^{(1)}(\mu_m) = \frac{4}{3} + L_m, \quad (15)$$

$$d^{(2)}(\mu_m) = \frac{3049}{288} + \frac{2}{9}\pi^2 + \frac{\pi^2}{9} \ln 2 - \frac{1}{6}\zeta_3 + \frac{173}{24}L_m + \frac{15}{8}L_m^2 - \left(\frac{71}{144} + \frac{1}{18}\pi^2 + \frac{13}{36}L_m + \frac{1}{12}L_m^2 \right) n_l - \left(\frac{143}{144} - \frac{1}{9}\pi^2 + \frac{13}{36}L_m + \frac{1}{12}L_m^2 \right) n_h, \quad (16)$$

where $L_m = 2 \ln \frac{\mu_m}{\overline{m}_c(\mu_m)}$.

Starting from Eq. (5), we can theoretically derive $f(r)$ in the $\overline{\text{MS}}$ mass scheme by formally converting m_c into $\overline{m}_c(\mu_m)$ using Eq. (15), and then expanding over α_s up to $\mathcal{O}(\alpha_s^2)$. It is worth noting that, while μ_m is formally arbitrary in principle, it is convenient to assign the same central values to both μ_m and μ_R , and then estimate the uncertainties by considering variations around these central values.

It is also important to note that we need to convert the m_c that explicitly appears in Eq. (3) and stems from the perturbative matching in the rest frame of the charmonium states. Clearly, it is not reasonable to choose μ_m to be related to the typical collision energy \sqrt{s} . Instead, it is natural to choose μ_m at $\mathcal{O}(m_c)$. In phenomenology, we choose $\mu_m = \overline{m}_c(\overline{m}_c)$.

V. EXAMINING THE CONVERGENT BEHAVIOUR OF THE ASYMPTOTIC EXPANSION

It is intriguing to investigate the convergence of the expansion in r for the $f^{(1)}$ and $f^{(2)}$. To facilitate this analysis, we first introduce a shorthand notation:

$$g_{a,b}^{(n)} = \sum_{i=0}^a \sum_{j=0}^b f_{i,j}^{(n)} r^i \ln^{2n-j} r. \quad (17)$$

Additionally, we employ $g_{\text{tot}}^{(n)}$ to represent the full contribution of $f^{(n)}$.

We begin our analysis with the NLO corrections. In Fig. 2, we present $f^{(1)}(r)$ as a function of r . The left panel compares the asymptotic expression with the full result for the real part of the $f^{(1)}$, while the right panel displays the imaginary part.

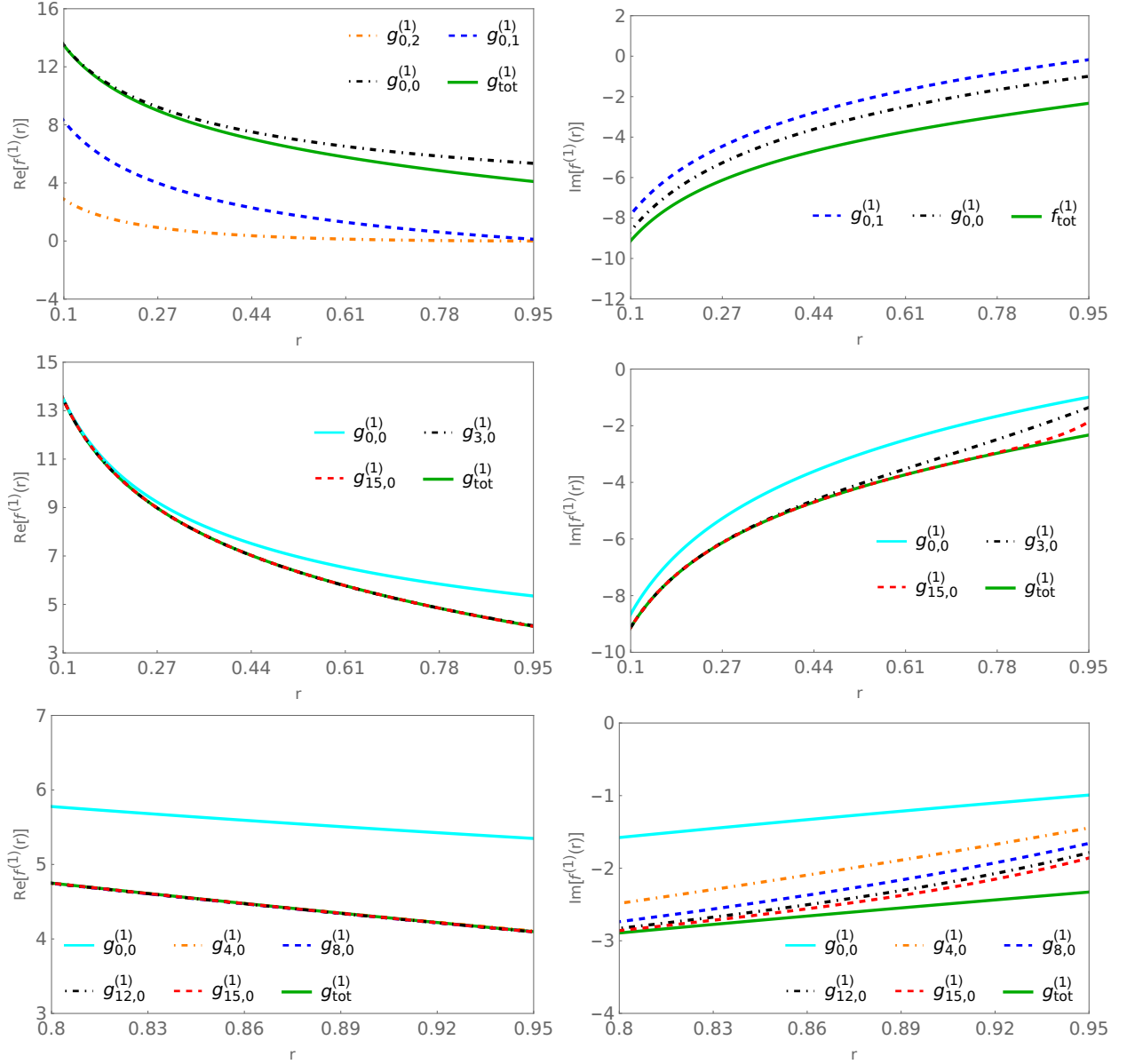


FIG. 2: Comparison of the asymptotic expressions with the full results for $f^{(1)}(r)$. The left panel shows the real part of $f^{(1)}(r)$, while the right panel shows the imaginary part of $f^{(1)}(r)$.

From the figure, several key observations can be made regarding the convergence behavior of the asymptotic expansion. For the real part, it is evident that the $r^0 \ln^2 r$ term alone significantly underestimates the full result¹. When the $r^0 \ln r$ term is included, the discrepancy between the asymptotic expression and the full result is substantially reduced. Further incorporation of the r^0 term brings the asymptotic expansion even closer to the full result, particularly for small values of $r < 0.3$. Moreover, the asymptotic expansion

¹ Notably, the definition of r in this work differs from that in Ref. [36], where r is defined as $4m_c^2/s$ and the $r^0 \ln^2 r$ term dominates $f^{(1)}$.

up to r^3 demonstrates remarkable agreement with the full result within the range $r < 1$. Specifically, the difference between the asymptotic expression and the full result remains below 1% even at $r = 0.99$. This indicates that the asymptotic expression for the real part of $f^{(1)}(r)$ exhibits excellent convergent behavior, providing a highly accurate approximation over a broad range of r values.

The convergence behavior of the imaginary part is notably less satisfactory compared to that of the real part. The leading logarithmic term for the imaginary part begins with $\ln r$. We observe that the asymptotic expansion up to r^0 already deviates significantly from the full result, even at $r = 0.1$. However, incorporating additional higher-order r terms into the expansion can gradually reduce this deviation. Specifically, the asymptotic expansion up to r^3 provides a reasonable approximation of the full result for $r < 0.5$, while extending the expansion up to r^{15} yields a good approximation for $r < 0.85$. Nevertheless, the convergence deteriorates rapidly as r increases beyond these ranges. For instance, the difference between the asymptotic expansion and the full result reaches 3% at $r = 0.85$, 8% at $r = 0.9$, and exceeds 20% at $r = 0.95$.

We now turn to the comparison at the NNLO level. In Fig. 3, we depict $f^{(2)}$ as a function of r , with the left and right panels corresponding to the real and imaginary parts of $f^{(2)}$, respectively. For the real part, it is noteworthy that the magnitude of the LO logarithmic term $r^0 \ln^4 r$ is significantly smaller than the full result². Despite this, the asymptotic expansion up to r^0 already provides a reasonable approximation to the full result for $r < 0.8$. However, the convergence deteriorates rapidly as r increases beyond 0.8. For instance, the difference between the asymptotic expression and the full result reaches 8% at $r = 0.85$, 17% at $r = 0.9$, and exceeds 40% at $r = 0.95$. More seriously, the difference between the full result and the asymptotic expansion up to r^{15} is even larger than that between the full result and the asymptotic expansion up to r^0 at $r > 0.85$. These observations highlight the poor convergence of the asymptotic expansion at large r values.

Similar to the real part, the asymptotic expansion for the imaginary part of $f^{(2)}$ demonstrates good convergent behavior for $r < 0.8$, while the convergence becomes poor for larger values of r . Specifically, the difference between the asymptotic expression and the full result reaches 6% at $r = 0.85$, 13% at $r = 0.9$, and exceeds 31% at $r = 0.95$. This is slightly better than the convergence observed for the real part of $f^{(2)}$.

It is worth noting that, although the convergence of the asymptotic expressions for the real part of $f^{(2)}$ and the imaginary parts of $f^{(1)}$ and $f^{(2)}$ remains poor for $r > 0.8$ near the threshold $s = 16m_c^2$, these expressions are still sufficient for making phenomenological predictions for the process $e^+e^- \rightarrow J/\psi + \eta_c$. In this context, r is expected to be much less than 1 to validate the applicability of the NRQCD factorization.

VI. PHENOMENOLOGY

Before making phenomenological predictions, we first specify the relevant input parameters. The masses of the J/ψ and η_c are taken from the latest Particle Data Group (PDG) [58]:

$$M_{J/\psi} = 3.096916 \text{ GeV}, \quad M_{\eta_c} = 2.9798 \text{ GeV}, \quad (18)$$

² In fact, even when using the definition $r = 4m_c^2/s$, the LO logarithmic term remains much smaller than the full result, which is in stark contrast to the NLO result. This discrepancy is attributed to the small coefficient associated with the $r^0 \ln^4 r$ term in $f^{(2)}$.

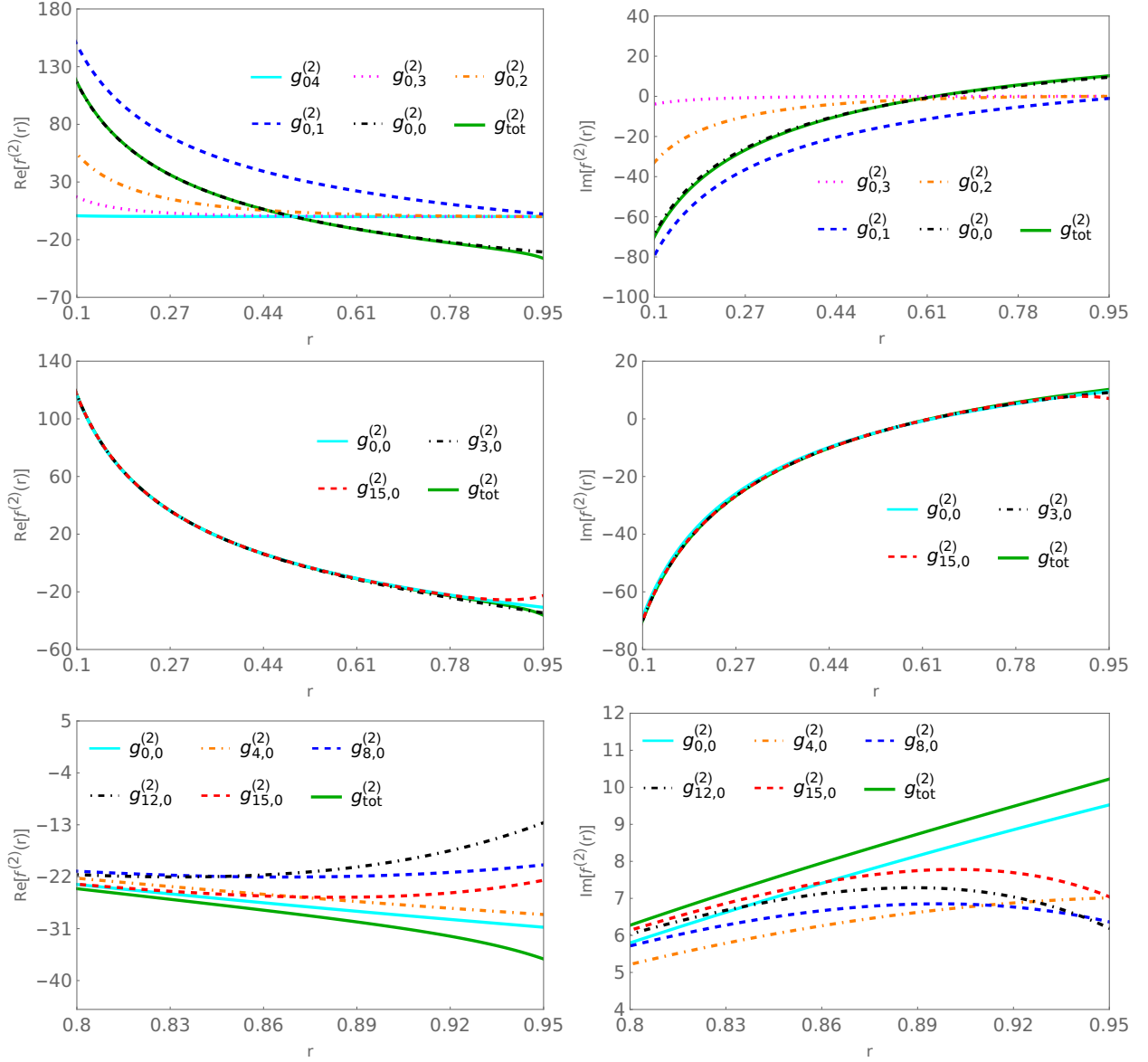


FIG. 3: Comparison of the asymptotic expressions with the full results for $f^{(2)}(r)$. The left panel shows the real part of $f^{(2)}(r)$, while the right panel shows the imaginary part of $f^{(2)}(r)$.

and the charm quark pole mass is set to $m_c = 1.5 \pm 0.2$ GeV. The NRQCD matrix elements are obtained from Ref. [19]:

$$\langle \mathcal{O} \rangle_{J/\psi} = 0.440 \text{ GeV}^3, \quad \langle \mathcal{O} \rangle_{\eta_c} = 0.437 \text{ GeV}^3, \quad (19)$$

which are fitted through the decays $J/\psi \rightarrow e^+e^-$ and $\eta_c \rightarrow \gamma\gamma$. The QED coupling constant is fixed to be $\alpha(\sqrt{s} = 10.6 \text{ GeV}) = 1/130.9$.

We also use the following input values [58]:

$$\alpha_s^{(n_f=5)}(M_Z) = 0.118, \quad \bar{m}_c^{(n_f=3)}(\bar{m}_c) = 1.273 \text{ GeV}, \quad (20)$$

and employ decoupling at flavor thresholds to convert these values to those with an active quark number $n_f = 4$. Using the RunDec package [59], the values of α_s and \bar{m}_c at other

energy scales are obtained by solving the renormalization group equations with $n_f = 4$. Additionally, we fix the factorization scale $\mu_\Lambda = 1$ GeV.

In Fig. 4, we present the theoretical predictions for the cross section as a function of the CM energy \sqrt{s} . The left panel and the right panel illustrate the predictions using the OS mass scheme and $\overline{\text{MS}}$ mass scheme, respectively. The shaded bands in the figures represent the uncertainties associated with varying the renormalization scale μ_R from $2m_c = 3.0$ GeV to \sqrt{s} , with the central value set at $\mu_R = \sqrt{s}/2$.

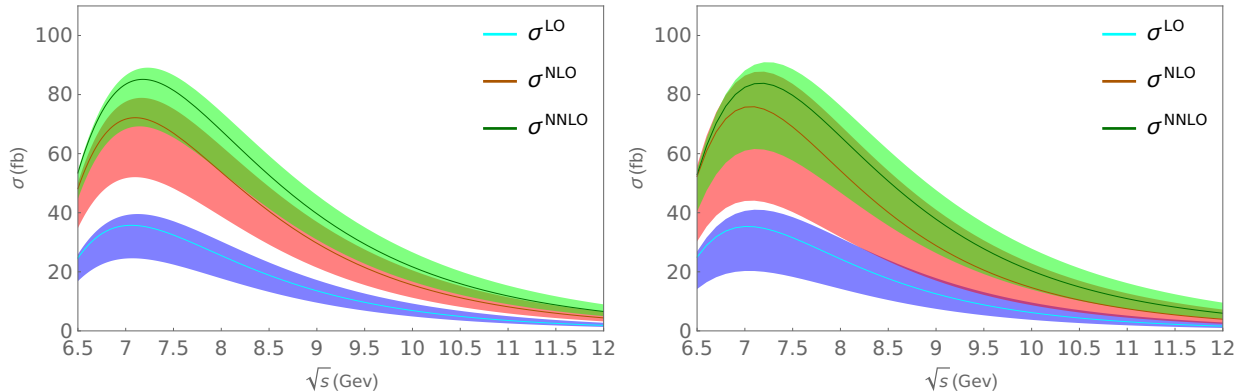


FIG. 4: The cross section as a function of \sqrt{s} at various levels of accuracy in α_s . The left panel corresponds to predictions from the OS mass scheme, while the right panel corresponds to predictions from the $\overline{\text{MS}}$ mass scheme. For the OS mass scheme prediction, We take $m_c = 1.5$ GeV. The shaded bands represent the uncertainty arising from varying μ_R from 3 GeV to \sqrt{s} .

From the figure, we can make several key observations. Firstly, the cross section calculated using the OS mass scheme is slightly larger than that obtained from the $\overline{\text{MS}}$ mass scheme. However, the shapes of the curves from both mass schemes are quite similar. Specifically, the cross section initially increases and then decreases with the increase of \sqrt{s} , reaching its maximum value at \sqrt{s} close to 7 GeV. It is worth noting that while the NRQCD factorization is not strictly valid at the lower end of the \sqrt{s} range and cannot provide fully reliable predictions, it still offers a reasonable theoretical estimate in this region.

Secondly, we observe that the perturbative corrections are substantial. Specifically, the $\mathcal{O}(\alpha_s^2)$ corrections are slightly smaller than the $\mathcal{O}(\alpha_s)$ corrections, particularly at lower values of \sqrt{s} .

Thirdly, we observe that the μ_R dependence of the predictions from the $\overline{\text{MS}}$ mass scheme is slightly larger than that from the OS mass scheme. This is somewhat counterintuitive and contrary to our initial expectations. In fact, a substantial portion of the uncertainty in the predictions from the $\overline{\text{MS}}$ mass scheme stems from the conversion of the pole mass m_c in the LO SDC (12)—which arises due to the helicity flip for the process $e^+e^- \rightarrow J/\psi + \eta_c$ —to the $\overline{\text{MS}}$ mass. In contrast, for helicity-conserved processes, the predictions from the $\overline{\text{MS}}$ mass scheme are expected smaller than those from the OS scheme.

In Table I, we present the cross section for the process $e^+e^- \rightarrow J/\psi + \eta_c$ at several specific values of \sqrt{s} , calculated using both the OS mass scheme and the $\overline{\text{MS}}$ mass scheme. The table includes uncertainties arising from the renormalization scale. Additionally, we account for the uncertainty in the charm quark mass within the OS mass scheme prediction by varying m_c from 1.3 to 1.7 GeV. It is found that the uncertainty stemming from the charm

TABLE I: The theoretical predictions for the cross section of the process $e^+e^- \rightarrow J/\psi + \eta_c$ are presented for both the OS and $\overline{\text{MS}}$ mass schemes. For the OS mass scheme, the uncertainties arise from two sources: varying μ_R from 3 GeV to \sqrt{s} , and varying the charm quark pole mass from 1.3 GeV to 1.7 GeV. For the $\overline{\text{MS}}$ mass scheme, the uncertainty is associated with varying μ_R from 3 GeV to \sqrt{s} .

$\sqrt{s}(\text{GeV})$	OS scheme			$\overline{\text{MS}}$ scheme		
	LO	NLO	NNLO	LO	NLO	NNLO
8	$25.5^{+4.8+8.4}_{-7.7-5.6}$	$53.7^{+8.8+23.9}_{-15.0-15.0}$	$67.8^{+6.3+35.7}_{-14.0-21.0}$	$24.2^{+7.0}_{-10.0}$	$52.9^{+14.9}_{-21.9}$	$63.7^{+9.2}_{-20.2}$
10.52	$4.8^{+1.8+1.6}_{-1.4-1.1}$	$11.1^{+4.0+4.8}_{-3.1-3.0}$	$15.8^{+4.2+7.9}_{-3.7-4.7}$	$4.3^{+2.6}_{-1.7}$	$10.1^{+6.3}_{-4.0}$	$14.2^{+5.9}_{-4.9}$
10.58	$4.7^{+1.8+1.5}_{-1.3-1.0}$	$10.7^{+3.9+4.6}_{-2.9-2.9}$	$15.2^{+4.1+7.6}_{-3.6-4.6}$	$4.1^{+2.5}_{-1.6}$	$9.7^{+6.1}_{-3.9}$	$13.7^{+5.7}_{-4.7}$
12	$1.9^{+0.9+0.6}_{-0.5-0.4}$	$4.4^{+2.1+1.9}_{-1.2-1.2}$	$6.6^{+2.4+3.3}_{-1.6-1.9}$	$1.6^{+1.2}_{-0.6}$	$3.9^{+3.2}_{-1.5}$	$5.8^{+3.4}_{-2.0}$

quark mass is comparable to, or even larger than, that from the renormalization scale, thus constituting one of the main sources of uncertainty for the OS mass scheme prediction. The cross sections obtained from the OS mass scheme are consistent with those from the $\overline{\text{MS}}$ scheme within the uncertainties.

Furthermore, it is evident that the cross section decreases rapidly with increasing CM energy. At $\sqrt{s} = 10.58$ GeV, our results are compatible with both the BELLE and BABAR experimental data within the uncertainties. It is worth noting that, with the formulas and expressions provided in the appendix and the attached file, one can easily calculate the cross sections at other CM energies.

VII. SUMMARY

In this work, we investigate the process $e^+e^- \rightarrow J/\psi + \eta_c$ using the NRQCD factorization framework. We present the SDCs up to NNLO in asymptotic expansions over $r = 16m_c^2/s$ up to r^{15} . Among these, the analytic expressions for some high-order logarithmic terms are obtained using the PSLQ algorithm. These expressions can be utilized for future theoretical studies, such as the resummation of logarithmic terms.

Although the asymptotic expressions eventually deviate from the full results near the threshold $r = 1$, the asymptotic expressions for the NLO and NNLO SDCs provide excellent approximations to the full results for $r < 0.8$, with deviations less than 3%. Notably, the difference between the asymptotic expression and the full result remains below 1% at $r = 0.99$ for the real part of the NLO SDC. Therefore, these asymptotic expressions can be reliably used for phenomenological predictions over a wide range of CM energies \sqrt{s} .

Additionally, we provide phenomenological predictions for the cross sections in both the OS mass scheme and the $\overline{\text{MS}}$ mass scheme. We investigate the uncertainty from the renormalization scale μ_R for the $\overline{\text{MS}}$ mass scheme, and account for uncertainties from both the μ_R and the charm quark mass in the OS mass scheme. The cross section as a function of \sqrt{s} is presented up to NNLO. We find that the μ_R uncertainty for predictions from the $\overline{\text{MS}}$ mass scheme is slightly larger than that from the OS scheme, which is largely attributed to the helicity flip in the process $e^+e^- \rightarrow J/\psi + \eta_c$. Finally, we observe that both mass schemes yield quite similar predictions, and our theoretical results are compatible with the available experimental data.

Acknowledgments

The work of C. Li. and W.-L. S. is supported by the National Natural Science Foundation of China under Grants No. 12375079, and the Natural Science Foundation of ChongQing under Grant No. CSTB2023 NSCQ-MSX0132. The work of X.-D. H. is supported by the Foundation of Chongqing Normal University under Grant No. 24XLB015.

Appendix A: Asymptotic expressions for NLO SDC

$$\begin{aligned}
f_{0,2}^{(1)} &= \frac{13}{24}, \\
f_{0,1}^{(1)} &= -\frac{41}{24} - \frac{11 \ln 2}{12} + \frac{13i\pi}{12}, \\
f_{0,0}^{(1)} &= -\frac{1}{6} + \frac{277 \ln 2}{24} - \frac{61 \ln^2 2}{24} - \frac{\pi^2}{36} + i \left(\frac{25\pi}{24} - \frac{11\pi \ln 2}{12} \right) - \left(\frac{5}{18} + \frac{i\pi}{6} \right) n_h \\
&\quad - \left(\frac{5}{18} + \frac{i\pi}{6} \right) n_l, \\
f_{1,2}^{(1)} &= \frac{23}{96}, \\
f_{1,1}^{(1)} &= -\frac{107}{192} + \frac{101 \ln 2}{96} + \frac{29i\pi}{48}, \\
f_{1,0}^{(1)} &= -\frac{43}{48} + \frac{459 \ln 2}{64} - \frac{321 \ln^2 2}{64} - \frac{49\pi^2}{192} - i \left(\frac{107\pi}{192} - \frac{77\pi \ln 2}{96} \right) - \frac{n_h}{4}, \\
f_{2,2}^{(1)} &= \frac{31}{192}, \\
f_{2,1}^{(1)} &= -\frac{4033}{3072} + \frac{123 \ln 2}{64} + \frac{43i\pi}{96} + \frac{n_h}{16}, \\
f_{2,0}^{(1)} &= -\frac{719}{4608} + \frac{7961 \ln 2}{768} - \frac{897 \ln^2 2}{128} - \frac{431\pi^2}{1152} - i \left(\frac{3841\pi}{3072} - \frac{107\pi \ln 2}{64} \right) \\
&\quad - \left(\frac{1}{32} + \frac{\ln 2}{8} - \frac{i\pi}{16} \right) n_h, \\
f_{3,2}^{(1)} &= \frac{109}{768}, \\
f_{3,1}^{(1)} &= -\frac{125389}{73728} + \frac{1907 \ln 2}{768} + \frac{151i\pi}{384} + \frac{n_h}{48}, \\
f_{3,0}^{(1)} &= \frac{16253}{147456} + \frac{56431 \ln 2}{4608} - \frac{13013 \ln^2 2}{1536} - \frac{2125\pi^2}{4608} - i \left(\frac{119053\pi}{73728} - \frac{1739\pi \ln 2}{768} \right) \\
&\quad + \left(\frac{1}{72} - \frac{\ln 2}{24} + \frac{i\pi}{48} \right) n_h,
\end{aligned} \tag{A1}$$

Appendix B: Asymptotic expressions for NNLO SDC

$$\begin{aligned}
f_{0,4}^{(2)} &= \frac{11}{432}, \\
f_{0,3}^{(2)} &= -\frac{275}{144} + \frac{419 \ln 2}{864} + \frac{11i\pi}{108} + \frac{13n_h}{216} + \frac{13n_l}{216}, \\
f_{0,2}^{(2)} &= \frac{3943}{576} + \frac{2695 \ln 2}{288} - \frac{1039 \ln^2 2}{288} - \frac{173\pi^2}{864} - i \left(\frac{11\pi}{4} - \frac{419\pi \ln 2}{288} \right) - \left(\frac{787}{1728} + \frac{37 \ln 2}{144} \right) n_h \\
&\quad - \left(\frac{787}{1728} + \frac{37 \ln 2}{144} \right) n_l - \left(\frac{5}{192} - \frac{5 \ln^2 2}{96} \right)_{lbl}, \\
f_{0,1}^{(2)} &= -(60.3367 - 26.2776i) + (4.8134 - 1.5263i)n_h + (4.8134 - 1.5263i)n_l \\
&\quad - (0.0148 + 0.0064i)_{lbl}, \\
f_{0,0}^{(2)} &= -(7.7964 - 31.0330i) - (0.8070 + 6.2668i)n_h - (7.0174 + 6.2668i)n_l \\
&\quad - (0.3940 - 0.5818i)n_h n_l - (0.1970 - 0.2909i)n_h^2 - (0.1970 - 0.2909i)n_l^2 \\
&\quad - (0.0732 + 0.0466i)_{lbl},
\end{aligned} \tag{B1}$$

$$f_{\frac{1}{2},0}^{(2)} = 4.1809, \tag{B2}$$

$$\begin{aligned}
f_{1,4}^{(2)} &= \frac{545}{18432} + \frac{n_h}{512}, \\
f_{1,3}^{(2)} &= -\frac{1217}{3456} - \frac{365 \ln 2}{13824} + \frac{329i\pi}{4608} + \left(\frac{13}{432} - \frac{\ln 2}{64} + \frac{i\pi}{128} \right) n_h + \frac{13n_l}{1728} - \left(\frac{5}{2304} - \frac{5 \ln 2}{768} \right)_{lbl}, \\
f_{1,2}^{(2)} &= -\frac{901}{6912} - \frac{63215 \ln 2}{13824} + \frac{5323 \ln^2 2}{3072} + \frac{373\pi^2}{55296} - i \left(\frac{47\pi}{72} - \frac{343\pi \ln 2}{4608} \right) - \left[\frac{7121}{27648} + \frac{5 \ln 2}{64} \right. \\
&\quad \left. - \frac{15 \ln^2 2}{256} + \frac{\pi^2}{256} - i \left(\frac{5\pi}{96} - \frac{3\pi \ln 2}{64} \right) \right] n_h + \left(\frac{1243}{27648} + \frac{23 \ln 2}{384} + \frac{i\pi}{192} \right) n_l \\
&\quad - \left[\frac{115}{2304} - \frac{425 \ln 2}{4608} - \frac{65 \ln^2 2}{3072} + \frac{5\pi^2}{3072} + i \left(\frac{5\pi}{768} - \frac{5\pi \ln 2}{256} \right) \right]_{lbl}, \\
f_{1,1}^{(2)} &= -(9.6456 - 2.8901i) + (2.2756 - 2.0824i)n_h + (0.8372 - 0.2833i)n_l \\
&\quad + (0.0711 + 0.0510i)_{lbl}, \\
f_{1,0}^{(2)} &= -(17.3475 + 2.2720i) - (1.7368 - 0.2164i)n_h + (1.4880 + 0.3547i)n_l \\
&\quad + (0.1389 + 0.2618i)n_h n_l + (0.1389 + 0.2618i)n_h^2 + (0.0867 + 0.3686i)_{lbl},
\end{aligned} \tag{B3}$$

$$f_{\frac{3}{2},0}^{(2)} = 2.2052, \tag{B4}$$

$$\begin{aligned}
f_{2,4}^{(2)} &= \frac{4907}{221184} + \frac{n_h}{1024} + \left(\frac{5}{6144} \right)_{\text{lbl}}, \\
f_{2,3}^{(2)} &= \frac{21523}{82944} - \frac{3679 \ln 2}{6912} + \frac{2441 i \pi}{55296} - \left(\frac{13}{3456} + \frac{\ln 2}{128} - \frac{i \pi}{256} \right) n_h - \frac{n_l}{864} \\
&\quad - \left(\frac{175}{12288} - \frac{5 \ln 2}{384} - \frac{5 i \pi}{1536} \right)_{\text{lbl}}, \\
f_{2,2}^{(2)} &= \frac{3952339}{884736} - \frac{173389 \ln 2}{11520} + \frac{110953 \ln^2 2}{18432} + \frac{2483 \pi^2}{110592} + i \left(\frac{4201 \pi}{6912} - \frac{6659}{4608} \pi \ln 2 \right) \\
&\quad - \left[\frac{342817}{884736} - \frac{41}{144} \ln 2 + \frac{15}{1024} \ln^2 2 + \frac{5 \pi^2}{512} + i \left(\frac{3 \pi}{128} + \frac{3 \pi \ln 2}{128} \right) \right] n_h - \left(\frac{1297}{884736} - \frac{1757 \ln 2}{9216} \right. \\
&\quad \left. - \frac{i \pi}{192} \right) n_l - \left[\frac{5}{2048} - \frac{6665}{49152} \ln 2 + \frac{65}{1536} \ln^2 2 + \frac{5 \pi^2}{1152} + i \left(\frac{175 \pi}{4096} - \frac{5 \pi \ln 2}{128} \right) \right]_{\text{lbl}}, \\
f_{2,1}^{(2)} &= -(11.4040 + 4.8655i) + (2.3650 - 0.8400i)n_h + (0.7881 + 0.2525i)n_l \\
&\quad - (0.0347 + 0.0654i)n_h n_l - (0.0347 + 0.0655i)n_h^2 + (0.2282 + 0.3802i)_{\text{lbl}}, \\
f_{2,0}^{(2)} &= (5.3535 - 4.7121i) - (2.5221 - 1.6789i)n_h - (0.1479 - 0.2200i)n_l \\
&\quad + (0.2711 + 0.0144i)n_h n_l + (0.3336 + 0.0144i)n_h^2 + (0.0800 + 0.3934i)_{\text{lbl}}, \tag{B5}
\end{aligned}$$

$$f_{\frac{5}{2},0}^{(2)} = 1.1870, \tag{B6}$$

$$\begin{aligned}
f_{3,4}^{(2)} &= \frac{57203}{3538944} + \frac{3n_h}{4096} + \left(\frac{5}{4096} \right)_{\text{lbl}}, \\
f_{3,3}^{(2)} &= \frac{103085}{110592} - \frac{758783 \ln 2}{442368} + \frac{24317 i \pi}{884736} - \left(\frac{167}{13824} + \frac{3 \ln 2}{512} - \frac{3 i \pi}{1024} \right) n_h + \frac{5n_l}{13824} \\
&\quad - \left(\frac{77695}{3538944} - \frac{35 \ln 2}{2048} - \frac{5 i \pi}{1024} \right)_{\text{lbl}}, \\
f_{3,2}^{(2)} &= -(1.9464 + 2.8882i) - (0.1402 + 0.1862i)n_h + (0.1375 + 0.0266i)n_l \\
&\quad + (0.0526 - 0.0953i)_{\text{lbl}}, \\
f_{3,1}^{(2)} &= -(5.3434 + 1.9676i) + (1.4000 - 0.5885i)n_h + (0.7083 + 0.4364i)n_l \\
&\quad - (0.0116 + 0.0218i)n_h n_l - (0.0428 + 0.0218i)n_h^2 + (0.2721 + 0.6332i)_{\text{lbl}}, \\
f_{3,0}^{(2)} &= -(1.6410 + 0.1515i) - (0.4717 - 0.3237i)n_h - (0.0827 - 0.1960i)n_l \\
&\quad + (0.0769 - 0.0207i)n_h n_l + (0.1358 - 0.1188i)n_h^2 + (0.1008 + 0.2279i)_{\text{lbl}} \tag{B7}
\end{aligned}$$

where the subscript *lbl* indicates the contribution from the lbl Feynman diagrams.

[1] K. Abe *et al.* [Belle], Phys. Rev. Lett. **89**, 142001 (2002) doi:10.1103/PhysRevLett.89.142001 [arXiv:hep-ex/0205104 [hep-ex]].

- [2] K. Abe *et al.* [Belle], Phys. Rev. D **70**, 071102 (2004) doi:10.1103/PhysRevD.70.071102 [arXiv:hep-ex/0407009 [hep-ex]].
- [3] B. Aubert *et al.* [BaBar], Phys. Rev. D **72**, 031101 (2005) doi:10.1103/PhysRevD.72.031101 [arXiv:hep-ex/0506062 [hep-ex]].
- [4] J. H. Yin *et al.* [Belle], JHEP **08**, 121 (2023) doi:10.1007/JHEP08(2023)121 [arXiv:2305.17947 [hep-ex]].
- [5] E. Braaten and J. Lee, Phys. Rev. D **67**, 054007 (2003) [erratum: Phys. Rev. D **72**, 099901 (2005)] doi:10.1103/PhysRevD.72.099901 [arXiv:hep-ph/0211085 [hep-ph]].
- [6] K. Y. Liu, Z. G. He and K. T. Chao, Phys. Lett. B **557**, 45-54 (2003) doi:10.1016/S0370-2693(03)00176-X [arXiv:hep-ph/0211181 [hep-ph]].
- [7] S. J. Brodsky, A. S. Goldhaber and J. Lee, Phys. Rev. Lett. **91**, 112001 (2003) doi:10.1103/PhysRevLett.91.112001 [arXiv:hep-ph/0305269 [hep-ph]].
- [8] K. Hagiwara, E. Kou and C. F. Qiao, Phys. Lett. B **570**, 39-45 (2003) doi:10.1016/j.physletb.2003.07.006 [arXiv:hep-ph/0305102 [hep-ph]].
- [9] K. M. Cheung and W. Y. Keung, Phys. Rev. D **69**, 094026 (2004) doi:10.1103/PhysRevD.69.094026 [arXiv:hep-ph/0311003 [hep-ph]].
- [10] J. P. Ma and Z. G. Si, Phys. Rev. D **70**, 074007 (2004) doi:10.1103/PhysRevD.70.074007 [arXiv:hep-ph/0405111 [hep-ph]].
- [11] A. E. Bondar and V. L. Chernyak, Phys. Lett. B **612**, 215-222 (2005) doi:10.1016/j.physletb.2005.03.021 [arXiv:hep-ph/0412335 [hep-ph]].
- [12] K. Y. Liu, Z. G. He and K. T. Chao, Phys. Rev. D **77**, 014002 (2008) doi:10.1103/PhysRevD.77.014002 [arXiv:hep-ph/0408141 [hep-ph]].
- [13] Y. J. Zhang, Y. j. Gao and K. T. Chao, Phys. Rev. Lett. **96**, 092001 (2006) doi:10.1103/PhysRevLett.96.092001 [arXiv:hep-ph/0506076 [hep-ph]].
- [14] V. V. Braguta, A. K. Likhoded and A. V. Luchinsky, Phys. Rev. D **72**, 074019 (2005) doi:10.1103/PhysRevD.72.074019 [arXiv:hep-ph/0507275 [hep-ph]].
- [15] G. T. Bodwin, D. Kang and J. Lee, Phys. Rev. D **74**, 114028 (2006) doi:10.1103/PhysRevD.74.114028 [arXiv:hep-ph/0603185 [hep-ph]].
- [16] D. Ebert and A. P. Martynenko, Phys. Rev. D **74**, 054008 (2006) doi:10.1103/PhysRevD.74.054008 [arXiv:hep-ph/0605230 [hep-ph]].
- [17] Z. G. He, Y. Fan and K. T. Chao, Phys. Rev. D **75**, 074011 (2007) doi:10.1103/PhysRevD.75.074011 [arXiv:hep-ph/0702239 [hep-ph]].
- [18] H. M. Choi and C. R. Ji, Phys. Rev. D **76**, 094010 (2007) doi:10.1103/PhysRevD.76.094010 [arXiv:0707.1173 [hep-ph]].
- [19] G. T. Bodwin, J. Lee and C. Yu, Phys. Rev. D **77**, 094018 (2008) doi:10.1103/PhysRevD.77.094018 [arXiv:0710.0995 [hep-ph]].
- [20] B. Gong and J. X. Wang, Phys. Rev. D **77**, 054028 (2008) doi:10.1103/PhysRevD.77.054028 [arXiv:0712.4220 [hep-ph]].
- [21] X. H. Guo, H. W. Ke, X. Q. Li and X. H. Wu, [arXiv:0804.0949 [hep-ph]].
- [22] E. Mengesha and S. Bhatnagar, Int. J. Mod. Phys. E **20**, 2521-2533 (2011) doi:10.1142/S0218301311030017 [arXiv:1105.4944 [hep-ph]].
- [23] H. R. Dong, F. Feng and Y. Jia, Phys. Rev. D **85**, 114018 (2012) doi:10.1103/PhysRevD.85.114018 [arXiv:1204.4128 [hep-ph]].
- [24] X. H. Li and J. X. Wang, Chin. Phys. C **38**, 043101 (2014) doi:10.1088/1674-1137/38/4/043101 [arXiv:1301.0376 [hep-ph]].
- [25] G. T. Bodwin, H. S. Chung and J. Lee, Phys. Rev. D **90**, no.7, 074028 (2014)

- doi:10.1103/PhysRevD.90.074028 [arXiv:1406.1926 [hep-ph]].
- [26] X. H. Li and J. X. Wang, Chin. Phys. C **38**, 043101 (2014) doi:10.1088/1674-1137/38/4/043101 [arXiv:1301.0376 [hep-ph]].
 - [27] Z. Sun, X. G. Wu, Y. Ma and S. J. Brodsky, Phys. Rev. D **98**, no.9, 094001 (2018) doi:10.1103/PhysRevD.98.094001 [arXiv:1807.04503 [hep-ph]].
 - [28] F. Feng, Y. Jia, Z. Mo, W. L. Sang and J. Y. Zhang, Phys. Lett. B **850**, 138506 (2024) doi:10.1016/j.physletb.2024.138506 [arXiv:1901.08447 [hep-ph]].
 - [29] L. Zeng, H. B. Fu, D. D. Hu, L. L. Chen, W. Cheng and X. G. Wu, Phys. Rev. D **103**, no.5, 056012 (2021) doi:10.1103/PhysRevD.103.056012 [arXiv:2102.01842 [hep-ph]].
 - [30] Z. Sun, JHEP **09**, 073 (2021) doi:10.1007/JHEP09(2021)073 [arXiv:2107.02047 [hep-ph]].
 - [31] X. D. Huang, B. Gong and J. X. Wang, JHEP **02**, 049 (2023) doi:10.1007/JHEP02(2023)049 [arXiv:2212.03631 [hep-ph]].
 - [32] G. T. Bodwin, E. Braaten and G. P. Lepage, Phys. Rev. D **51**, 1125-1171 (1995) [erratum: Phys. Rev. D **55**, 5853 (1997)] doi:10.1103/PhysRevD.55.5853 [arXiv:hep-ph/9407339 [hep-ph]].
 - [33] M. Beneke and V. M. Braun, Nucl. Phys. B **426**, 301-343 (1994) doi:10.1016/0550-3213(94)90314-X [arXiv:hep-ph/9402364 [hep-ph]].
 - [34] I. I. Y. Bigi, M. A. Shifman, N. G. Uraltsev and A. I. Vainshtein, Phys. Rev. D **50**, 2234-2246 (1994) doi:10.1103/PhysRevD.50.2234 [arXiv:hep-ph/9402360 [hep-ph]].
 - [35] M. Beneke, Phys. Lett. B **344**, 341-347 (1995) doi:10.1016/0370-2693(94)01505-7 [arXiv:hep-ph/9408380 [hep-ph]].
 - [36] Y. Jia, J. X. Wang and D. Yang, JHEP **10**, 105 (2011) doi:10.1007/JHEP10(2011)105 [arXiv:1012.6007 [hep-ph]].
 - [37] A. Czarnecki and K. Melnikov, Phys. Rev. Lett. **80**, 2531-2534 (1998) doi:10.1103/PhysRevLett.80.2531 [arXiv:hep-ph/9712222 [hep-ph]].
 - [38] M. Beneke, A. Signer and V. A. Smirnov, Phys. Rev. Lett. **80**, 2535-2538 (1998) doi:10.1103/PhysRevLett.80.2535 [arXiv:hep-ph/9712302 [hep-ph]].
 - [39] A. Czarnecki and K. Melnikov, Phys. Lett. B **519**, 212-218 (2001) doi:10.1016/S0370-2693(01)01129-7 [arXiv:hep-ph/0109054 [hep-ph]].
 - [40] T. Hahn, Comput. Phys. Commun. **140**, 418-431 (2001) doi:10.1016/S0010-4655(01)00290-9 [arXiv:hep-ph/0012260 [hep-ph]].
 - [41] R. Mertig, M. Bohm and A. Denner, Comput. Phys. Commun. **64**, 345-359 (1991) doi:10.1016/0010-4655(91)90130-D
 - [42] F. Feng and R. Mertig, [arXiv:1212.3522 [hep-ph]].
 - [43] M. Beneke and V. A. Smirnov, Nucl. Phys. B **522**, 321-344 (1998) doi:10.1016/S0550-3213(98)00138-2 [arXiv:hep-ph/9711391 [hep-ph]].
 - [44] The package CalcLoop: <https://gitlab.com/multiloop-pku/calclloop>.
 - [45] J. Klappert, F. Lange, P. Maierhöfer and J. Usovitsch, Comput. Phys. Commun. **266**, 108024 (2021) doi:10.1016/j.cpc.2021.108024 [arXiv:2008.06494 [hep-ph]].
 - [46] X. Guan, X. Liu, Y. Q. Ma and W. H. Wu, Comput. Phys. Commun. **310**, 109538 (2025) doi:10.1016/j.cpc.2025.109538 [arXiv:2405.14621 [hep-ph]].
 - [47] A. V. Smirnov, Comput. Phys. Commun. **189**, 182-191 (2015) doi:10.1016/j.cpc.2014.11.024 [arXiv:1408.2372 [hep-ph]].
 - [48] X. Liu, Y. Q. Ma and C. Y. Wang, Phys. Lett. B **779**, 353-357 (2018) doi:10.1016/j.physletb.2018.02.026 [arXiv:1711.09572 [hep-ph]].
 - [49] Z. F. Liu and Y. Q. Ma, Phys. Rev. Lett. **129**, no.22, 222001 (2022)

- doi:10.1103/PhysRevLett.129.222001 [arXiv:2201.11637 [hep-ph]].
- [50] X. Liu and Y. Q. Ma, Comput. Phys. Commun. **283**, 108565 (2023) doi:10.1016/j.cpc.2022.108565 [arXiv:2201.11669 [hep-ph]].
 - [51] W. L. Sang, F. Feng, Y. Jia, Z. Mo and J. Y. Zhang, Phys. Lett. B **843**, 138057 (2023) doi:10.1016/j.physletb.2023.138057 [arXiv:2202.11615 [hep-ph]].
 - [52] W. L. Sang, F. Feng, Y. Jia, Z. Mo, J. Pan and J. Y. Zhang, Phys. Rev. Lett. **131**, no.16, 161904 (2023) doi:10.1103/PhysRevLett.131.161904 [arXiv:2306.11538 [hep-ph]].
 - [53] N. Gray, D. J. Broadhurst, W. Grafe and K. Schilcher, Z. Phys. C **48**, 673-680 (1990) doi:10.1007/BF01614703
 - [54] J. Fleischer, F. Jegerlehner, O. V. Tarasov and O. L. Veretin, Nucl. Phys. B **539**, 671-690 (1999) [erratum: Nucl. Phys. B **571**, 511-512 (2000)] doi:10.1016/S0550-3213(98)00705-6 [arXiv:hep-ph/9803493 [hep-ph]].
 - [55] K. G. Chetyrkin and M. Steinhauser, Nucl. Phys. B **573**, 617-651 (2000) doi:10.1016/S0550-3213(99)00784-1 [arXiv:hep-ph/9911434 [hep-ph]].
 - [56] K. Melnikov and T. v. Ritbergen, Phys. Lett. B **482**, 99-108 (2000) doi:10.1016/S0370-2693(00)00507-4 [arXiv:hep-ph/9912391 [hep-ph]].
 - [57] P. Marquard, A. V. Smirnov, V. A. Smirnov, M. Steinhauser and D. Wellmann, Phys. Rev. D **94**, 074025 (2016) doi:10.1103/PhysRevD.94.074025 [arXiv:1606.06754 [hep-ph]].
 - [58] S. Navas *et al.* [Particle Data Group], Phys. Rev. D **110**, 030001 (2024) doi:10.1103/PhysRevD.110.030001
 - [59] K. G. Chetyrkin, J. H. Kuhn and M. Steinhauser, Comput. Phys. Commun. **133**, 43-65 (2000) doi:10.1016/S0010-4655(00)00155-7 [arXiv:hep-ph/0004189 [hep-ph]].